Dynamics of globally coupled inhibitory neurons with heterogeneity

David Golomb and John Rinzel
Mathematical Research Branch, National Institute of Diabetes and Digestive and Kidney Diseases, Building 31, Room 4B-54, National Institutes of Health, Bethesda, Maryland, 20892
(Received 11 March 1993)

A model of many heterogeneous excitable neurons with a global slowly decaying inhibitory coupling is studied. When neuronal intrinsic excitability parameters are randomly distributed, the system exhibits four regimes of behavior. In addition to synchronized periodic and asynchronous regimes, we obtain two aperiodic regimes, with bursting rate a staircaselike function of neuron excitability. In one regime, the system is partially synchronized and, in the second, partially antisynchronized. The transition between these two regimes is discontinuous as the disorder increases.

PACS number(s): 87.10.+e, 05.45.+b

Recent studies have considered the dynamics of many globally coupled oscillators [1–6]. Most efforts have treated "generic" models, with or without quenched disorder (i.e., parametric heterogeneity), in which each unit's state is represented by a phase [1–5] or by a complex number [6]. In these models, an isolated unit oscillates periodically, and the effects of coupling on the individual oscillators are investigated. Many studies have treated *weak* coupling since then the system dynamics are reducible to a phase model [1,7]. For our case, of a realistic Hodgkin-Huxley-type neuron model, coupling is not weak. Moreover, an uncoupled, unstimulated element is not an oscillator, but converges to a fixed point (FP), and oscillations emerge as a *collective* network effect. Here, phase reduction is inappropriate and new types of behavior are found.

Of additional importance is that, generally, in physical and especially biological systems the units are not identical. We study the quenched disorder effects on the dynamics of such globally coupled systems. In particular, we consider a model in which an uncoupled neuron has a stable rest state, but the globally coupled many-cell network of identical cells can oscillate due to inhibitory coupling which increases fast and decays slowly (but is not uniformly slow). Wang and Rinzel [8] demonstrated that oscillations of a small population of (2–10) identical neurons can arise and be synchronous when the inhibitory synapses decay slowly and the coupling is strong enough. This finding, later generalized for the case of a large network [9], countered the classical view that mutual inhibition does not cause in-phase oscillations.

In this article, heterogeneity is introduced in the neuron intrinsic properties. Increasing the level of heterogeneity changes the network behavior, and transitions analogous to phase transitions in statistical mechanics are observed. At low variability, the system is still periodic and synchronized, while at large variability the system converges to a stationary asynchronous state [6,3]. At intermediate variability, two regimes, characterized by a staircaselike dependence of the bursting rate on the cell excitability parameter, are seen. In one of them the network dynamics is synchronous and in the second it is antisynchronous. A sharp transition between these two regimes, characterized by a discontinuity in the system order parameters, is observed as the level of disorder crosses a critical value.

A single neuron in the system of N globally coupled (all-to-all) neurons is described by a set of three nonlinear differential equations, developed by Wang and Rinzel [8]. The model considers only two ionic currents (calcium and leakage). This model describes the slow voltage wave that underlies bursts of fast spikes, although spikes *per se* are not included here; it idealizes a neuron in a part of the brain called the reticular thalamic nucleus (RTN) [10]. The ith neuron, $i = 1, \ldots, N$ is characterized by three state variables: the membrane potential V_i, an auxiliary variable h_i, and the synaptic variable s_i. Neuronal dynamics are governed by the three differential equations

$$\frac{dV_i}{dt} = H_i(V_i, h_i) - g_{\mathrm{syn}}(V_i - V_{\mathrm{syn}})\, S(t) \ , \tag{1}$$

$$\frac{dh_i}{dt} = k_h(V_i)\,[h_\infty(V_i) - h_i] \ , \tag{2}$$

$$\frac{ds_i}{dt} = k_f s_\infty(V_i)\,(1 - s_i) - k_r s_i \ , \tag{3}$$

where the total inhibition order parameter $S(t)$, in this case of all-to-all coupling, is

$$S(t) = \frac{1}{N}\sum_{i=1}^{N} s_i(t) \ . \tag{4}$$

The nonlinear functions in Eqs. (1)–(3) are defined by

$$H(V,h) = -g_{\mathrm{Ca}i} m_\infty^3(V)\, h\,(V - V_{\mathrm{Ca}}) - g_L(V - V_L) \ , \tag{5}$$

with $m_\infty(V) = \Gamma(V, \theta_m, \sigma_m)$, $h_\infty(V) = \Gamma(V, \theta_h, \sigma_h)$, and $s_\infty(V) = \Gamma(V, \theta_s, \sigma_s)$, where

$$\Gamma(V, \theta, \sigma) = \{1 + \exp[-(V - \theta)/\sigma]\}^{-1} \ . \tag{6}$$

The rate function in Eq. (2) is $k_h(V) = \phi \exp[-(V - \theta_{hk})/\sigma_{hk}]/h_\infty(V)$. These equa-

tions are nondimensionalized [11]. An uncoupled neuron ($g_{\rm syn} = 0$) with $g_{\rm Ca} = 1$ has a globally attracting FP, the rest state.

Equations (1)–(4) define a $3N$-dimensional dynamical system, whose behavior is of interest for large time and large N. The self-coupling term ($i = j$) in Eq. (1) simplifies the analysis and is negligible for large N. For describing the system's behavior, we define the population-averaged voltage $V(t) = (1/N)\sum_{i=1}^{N} V_i(t)$ and the time-averaged quantities, $\bar{V} = \langle V(t)\rangle$, $\bar{S} = \langle S(t)\rangle$, and ${\sigma_V}^2 = \langle (V(t) - \bar{V})^2 \rangle$, where $\langle\,\rangle$ denotes time averaging after the system has converged to an attractor. The time-averaged voltage fluctuation σ_V represents the degree of synchronization. It is zero for a totally asynchronous system.

In the case of a homogeneous network, i.e., $g_{{\rm Ca}i} = \bar{g}_{\rm Ca}$, the system is symmetric to permuting the neurons. Hence, the homogeneous solution always exists, and for a specific choice of parameters it can be a homogeneous fixed point (HFP), a homogeneous limit cycle (HLC) (the synchronous phase-locked oscillation), or both. In addition, cluster states [9,3], in which the system spontaneously breaks into a small number of macroscopic clusters, may also appear. Here, we consider the regime of small k_r and large enough $g_{\rm syn}$, so that the HLC is the global attractor at large N. The effects of heterogeneity, which preclude the existence of the HFP, HLC and spontaneously broken cluster states, are investigated. Our results are based on numerical computation. The initial conditions for V_i were chosen at random, while h_i and s_i were initialized with the steady-state value of the corresponding V_i.

Most of the parameters that define the model are determined by the biophysics of the ionic currents and do not vary considerably among neurons of a given type. Parameters that likely do vary include $g_{\rm Ca}$, g_L, and $g_{\rm syn}$, which relate to the total number of ionic channels per cell. In the limit of large N, a random distribution of $g_{\rm syn}$ will be averaged out, and the important variabilities will be those of $g_{\rm Ca}$ and g_L. Here we have chosen to examine the heterogeneity of only one parameter, $g_{\rm Ca}$, which is our excitability parameter. Simulations show that the effect of altering g_L is similar.

We consider the case where $g_{{\rm Ca}i}$ has its values chosen from a *uniform* distribution $\rho(g_{\rm Ca})$ with average 1 and standard deviation σ_g. The values of σ_V and $\bar{S}$, obtained from numerical simulation, are presented in Fig. 1. Four regimes of behavior are seen as σ_g increases. For small σ_g, the system still converges to a limit cycle. For large σ_g, it reaches a stationary state characterized by asynchrony for oscillating cells, and in between there are two regimes of aperiodic behavior. Each neuron's average bursting rate f_b and phases of bursting are shown in Fig. 2 for several values of σ_g. These regimes are described as follows.

Periodic state (P): $0 \le \sigma_g \lesssim 0.014$. For small values of σ_g, the system remains periodic (in contrast to populations of integrate-and-fire neuron models that do not fully synchronize as heterogeneiety vanishes [12]). All the neurons burst in synchrony, each emitting one burst per cycle. The bursting phase depends on $g_{\rm Ca}$ such that low-$g_{\rm Ca}$ neurons burst later. The peak voltage increases with $g_{\rm Ca}$.

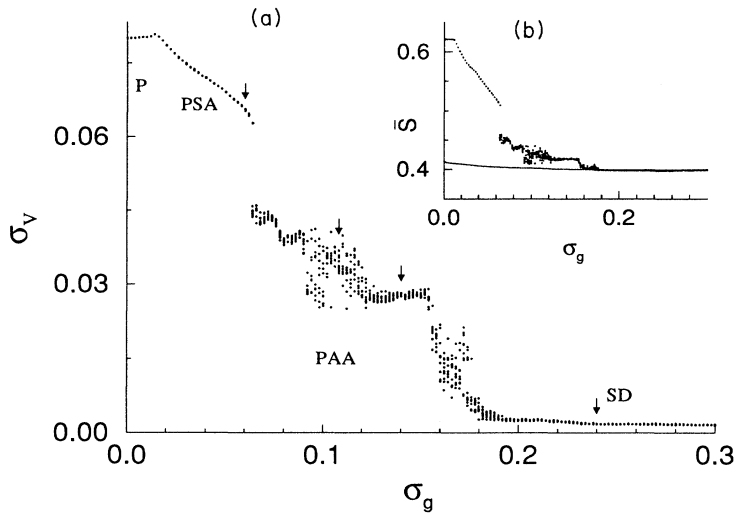

FIG. 1. Time-averaged order parameters, calculated from simulations with $N = 1000$ and averaged over the last half of 1.25×10^4 time units, vs σ_g: voltage fluctuations σ_V in (a); total inhibition $\bar{S}$ in (b). Ten different sets of random initial conditions were used for each value of σ_g. Four regimes are seen: P, periodic; PSA, partially synchronous aperiodic; PAA, partially antisynchronous aperiodic (here, multiple data points for given σ_g show that different attractors were obtained for different initial conditions); SD, stationary distribution. The nonzero σ_V in the SD regime is a finite size effect. The arrows indicate the σ_g values chosen in Fig. 2. In (b) the solid curve represents the constant $S_{\rm SD}$ for the SD state, calculated from Eqs. (7) and (8). Numerical integrations of Eqs. (1)–(3) performed with the second-order Runge-Kutta method ($\delta t = 0.25$).

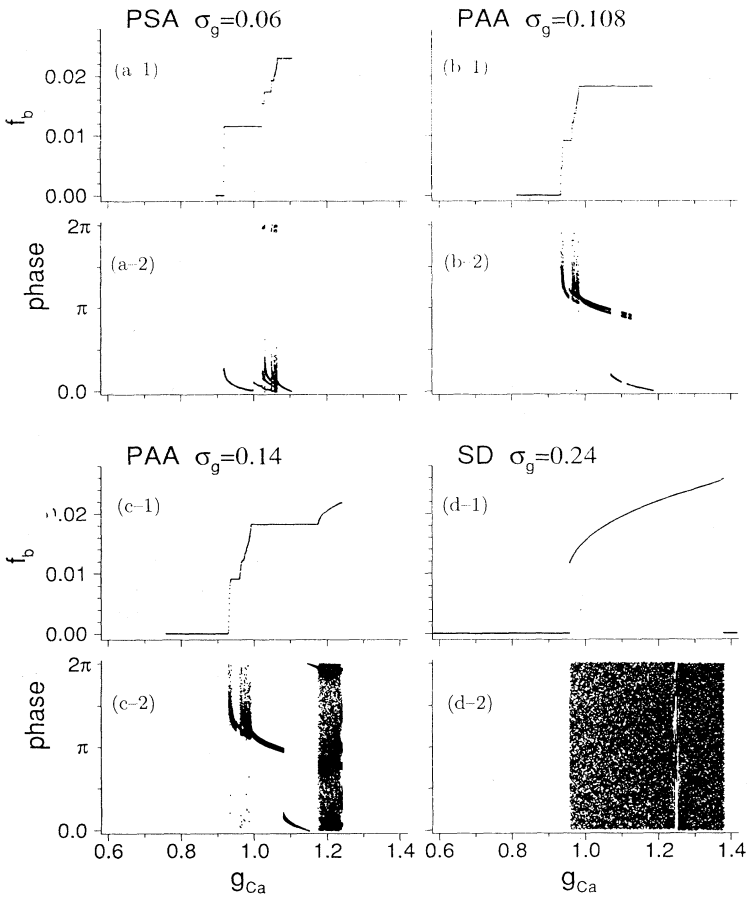

FIG. 2. The bursting rates f_b and phases of neurons vs g_{Ca} for four different amounts of variability σ_g [arrows in Fig. 1(a)]. If a neuron's voltage peak at time t_i exceeds $\theta_{syn} = -0.375$ we say a burst occurred at t_i. The bursting rate is the time-averaged number of bursts per second. Phase is measured relative to the burst cycles of one neuron (label g'_{Ca}) chosen as the clock. Staircaselike structure of f_b is observed in the PSA and PAA regimes: (a) $\sigma_g = 0.06$ (PSA regime), $g_{Ca}{}' = 1.104$; (b) $\sigma_g = 0.108$ (PAA regime), $g_{Ca}{}' = 1.186$; (c) $\sigma_g = 0.14$ (PAA regime), $g_{Ca}{}' = 1.146$ (here, the phases of the highest-g_{Ca} neurons tend to accumulate around 0 and π). Notice that within a group of neurons having constant f_b there may be subgroups of distinctly different phases. Asynchronous behavior for the SD regime is seen in panels (d) with $\sigma_g = 0.24$, $g_{Ca}{}' = 1.248$. Here, f_b vs g_{Ca} matches well the behavior of the self-consistent solution with $S_{SD} = 0.3891$, as computed from Eqs. (7) and (8).

Stationary distribution (SD): $\sigma_g \gtrsim 0.175$ [6,3,13,14]. In this state, population-averaged variables, in particular $S(t)$ and $V(t)$, are constant in time. Since S is constant, the dynamics of each neuron is determined by the two-dimensional vector field [Eqs. (1) and (2)], where S is determined self-consistently by Eqs. (3) and (4). Low-g_{Ca} neurons are quiescent ($f_b = 0$) at low voltage, high-g_{Ca} neurons are steady at high voltage, and intermediate-g_{Ca} (g_{Ca} not too different from 1) oscillate periodically and asynchronously [Fig. 2(d-1)]. There is a small regime of bistability for neurons with g_{Ca} near 1.4; they approach either a FP or a limit cycle (LC) depending on the initial conditions. The stationary distribution is obtained only in the limit $N \to \infty$. For finite N, the global order parameters fluctuate chaotically with decaying amplitude that scales like $1/\sqrt{N}$, for σ_g far from the transition [4,6,13].

The total-inhibition order parameter S_{SD} of the SD is calculated self-consistently as follows. Assume a value S for it and calculate the neurons' trajectories. Since S is time independent, there are no phase relations between different neurons on different limit cycles [Fig. 2(d-2)]. Thus, we use the random-phase-approximation ansatz [5,6] and assume that each neuron on a limit cycle contributes to the inhibitory field only through the time average of its $s_i(t)$. Assuming S and denoting the temporal period of a neuron by $T(g_{Ca}, S)$, we calcuate the self-consistent value of S, denoted by S_{cal}, by averaging $s_i(t)$ over the time period and over the population:

$$S_{cal}(S) = \int dg_{Ca}\, \rho(g_{Ca}) \frac{1}{T(g_{Ca}, S)} \int_0^{T(g_{Ca},S)} dt\, s_i(t) \quad . \tag{7}$$

For the neurons that go to a FP, $T(g_{Ca}, S)$ is arbitrary. The self-consistent solution S_{SD} then satisfies the equation

$$S_{cal}(S_{SD}) = S_{SD} \quad . \tag{8}$$

Since even for a specific S_{SD} there are bistable neurons that can go either to a FP or to a LC, the value of S_{cal} is not uniquely determined, and there is a range of values that can be obtained. This means that there can be a continuum of SD states. However, this regime of possible S is generally small and all the SD states are similar. The selection of the SD is based on stability and basin-of-attraction considerations, not analyzed here. Our calculations show that S_{SD} is only slightly dependent on σ_g [Fig. 1(b)]. The self-consistently calculated value of S (not shown) agrees well with the simulation results [Fig. 1(b)], in the regime where the SD state is the stable attractor. The SD solution exists for each finite σ_g, but is not stable at low variability.

Partially synchronous aperiodic (PSA) regime: $0.014 \lesssim \sigma_g \lesssim 0.064$. The network is aperiodic, but its behavior is characterized by a fundamental frequency f_0 and time period $T_0 = 1/f_0$, corresponding to a peak in the Fourier spectrum of $V(t)$. The neuron trajectories reveal a high degree of synchronization with this frequency. High-g_{Ca} neurons burst almost periodically in a synchronized manner. Their amplitude increases with g_{Ca}, and for each neuron the amplitude of consecutive oscillations is almost constant in time. Their bursting rate f_b equals f_0. As the excitability parameter g_{Ca} decreases through the population, f_b decreases monotonically [Fig. 2(a-1)], in stepwise fashion. Each step represents a group of neurons with the same f_b. Prominent steps are seen at rational multipliers of f_0. Notice especially that many neurons burst at $f_b = f_0/2$, but that this group consists of two subgroups bursting alternately. Neurons with low enough g_{Ca} do not burst at all. Nearly all the bursts occur within a small fraction of the period [$\sim 0.15T_0$ for $\sigma_g = 0.06$, see Fig. 2(a-2)], implying high, but not full, synchronization. The low-g_{Ca} neurons oscillate with frequency f_0, but the amplitude of consecutive cycles varies and repeats itself approximately only after an integer number of T_0, which differs from cell to cell. For these neurons $f_b < f_0$ since the voltage peaks in many cycles fall below the threshold (-0.375) for our definition of "bursting." The number of neurons with $f_b = f_0$ decreases as σ_g increases, but remains finite below the transition which terminates this PSA regime.

Partially antisynchronous aperiodic (PAA) regime: $0.064 \lesssim \sigma_g \lesssim 0.175$. The network is aperiodic, presumably chaotic. Depending on initial conditions, the system converges to different attractors, characterized by different time-averaged quantities like $\bar{V}$, σ_V, and $\bar{S}$, and different fundamental frequencies f_0. The high-g_{Ca} neurons divide into two or three groups, depending on σ_g and the particular attractor. Two groups of high-g_{Ca} neurons burst alternately every $\sim 2T_0$. Neurons within each group burst in synchrony, within a small fraction of the time period [Figs. 2(b-2) and 2(c-2)]. The phase difference between the groups is around π, and they are close to being antisynchronous. A third group, containing the highest-g_{Ca} neurons, may also exist, especially for large σ_g [Fig. 2(c-2)]. The f_b of these neurons exceeds that of neurons in the two other groups and increases continuously with g_{Ca}. Although the cells can burst at any phase, they are more likely to burst around 0 or π. The steplike structure of f_b is observed also in this regime [Figs. 2(b-1) and 2(c-1)], and large groups of neurons with $f_b = 0$ (quiescent) and $f_b = f_0/2$ are found. The quiescent low-g_{Ca} neurons show small fluctuations with frequency f_0 around their steady inhibited level. Neurons with intermediate values of g_{Ca} burst every few fundamental periods in an irregular manner.

The bursting rate steps found in the PSA and PAA regimes are similar to those of the devil's staircase found for phase-locking behavior of periodically forced oscillators in physical systems (e.g., Josephson junctions) and in biological systems (e.g., neural pacemakers) [15]. They represent the effects of frequency-locking, and sometimes also phase-locking, among groups of neurons within the population. Frequency plateaus can develop along a chain of endogenous oscillators (nearest neighbor coupling) when the gradient of intrinsic frequencies is too large ([16]). However, plateaus have not been reported for globally coupled disordered systems without external periodic forcing; for example, not in a model of coupled Ginzburg-Landau units ([6]).

One expects that our system's synchrony should deteriorate as the disorder σ_g increases, as found also in "generic" models [1,2,6]. Our simulations (Fig. 1) clearly show the transitions from the P (periodic) to PSA regimes and from the PSA to PAA regimes. During the first transition (P to PSA) the order parameter $\bar{S}$ changes continuously with σ_g. In the second transition (PSA to PAA) it jumps discontinuously as the disorder σ_g increases. This unexpected sharp transition between a partially synchronized phase to partially antisynchronized phase is a novel result of our model and has not been observed in other models of disordered systems. The transition from the PAA to SD regime is smeared out in the simulation. A rigorous linear stability theory of the SD state is needed in order to better understand this transition.

In summary, we have demonstrated that heterogeneity of the cell population strongly affects the system's dynamics. Although the periodic state, in which all the neurons are phase-locked with slight phase differences is the global attractor at very small variability, the amount of variability needed to break the full synchrony is relatively small. At intermediate variability the system behaves aperiodically; the bursting rate of neurons in a given network increases in steplike fashion with cell excitability, g_{Ca}. This staircase structure has not been observed in other models of globally coupled oscillators. Two regimes at different σ_g ranges are discovered with a sharp transition between them. In one, the neurons are partially synchronized, and in the second (larger σ_g) they are partially antisynchronized. At sufficiently high variability, the system converges to a stationary distribution state that is composed of periodic and stationary neurons.

In further computations (not shown here) we found that with stronger coupling (larger g_{syn}) the system tolerates greater variability before synchrony breaks down; the transitions P to PSA to PAA to SD are shifted to higher σ_g values. The sharp transition and the staircase structure appear for intermediate variability and inhibitory coupling that is slowly decaying and not weak. These features are qualitative, not sensitive to the particular parameters of the model. Moreover, if the synaptic decay rate is too rapid (say, $k_r = 0.1$, $g_{\mathrm{syn}} = 0.7$) the regimes P and PSA do not occur. We conclude that the *slow* decay of the inhibitory coupling is a significant factor for the existence of the synchronized regimes (consistent with Wang and Rinzel [8]) and for the sharp transition between the PSA and PAA regimes.

The model predicts that in the PAA regimes there are neurons that can be either in or out of phase, depending on the initial conditions. This prediction is consistent with recent experiments [17], where cross correlation between RTN neurons revealed both in-phase and 180° out-

of-phase synchronization. Although the RTN is a part of a larger feedback system, phase differences observed there may correspond to the PAA regime and may result from neuron variability.

We are grateful to D. Hansel, I. Segev, H. Sompolinsky, and X.-J. Wang for helpful discussions. We acknowledge computer time provided by the National Cancer Institute Biomedical Supercomputing Center.

[1] Y. Kuramoto, *Chemical Oscillations, Waves and Turbulence* (Springer, New York, 1984).
[2] Y. Kuramoto and I. Nishikawa, J. Stat. Phys. **49**, 569 (1987).
[3] D. Golomb, D. Hansel, B. Shraiman, and H. Sompolinsky, Phys. Rev. A **45**, 3516 (1992).
[4] H. Daido, J. Phys. A **20**, L629 (1987); Prog. Theor. Phys. **81**, 727 (1989); J. Stat. Phys. **60**, 753 (1990).
[5] S.H. Strogatz and R.E. Mirollo, J. Stat. Phys. **63**, 613 (1991).
[6] P.C. Matthews and S.H. Strogatz, Phys. Rev. Lett. **65**, 1701 (1990); P.C. Matthews, R.E. Mirollo, and S.H. Strogatz, Physica D **52**, 293 (1991).
[7] D. Hansel, G. Mato, and C. Meunier, Europhys. Lett. **23**, 367 (1993); Phys. Rev. E (to be published).
[8] X.J. Wang, J. Rinzel, and M.A. Rogawski, J. Neurophysiol. **66**, 839 (1991); X.J. Wang and J. Rinzel, Neural Computation **4**, 84 (1992); Neuroscience **53**, 899 (1993).
[9] D. Golomb and J. Rinzel, Physica D (to be published).
[10] According to Steriade and colleagues, the brain's RTN serves as pacemaker for synchronous oscillations (7–14 Hz) seen during drowsiness sleep or anesthesia. See M. Steriade, L. Domich, G. Oakson, and M. Deschenes, J. Neurophysiol. **57**, 260 (1987); C. Mulle, A. Madariaga, and M. Deschenes, J. Neuroscience **6**, 2134 (1986).
[11] The equations of Wang and Rinzel were nondimensionalized as follows. Voltages were divided by the previously dimensioned $V_{\mathrm{Ca}} = 120$ mV, conductances by the previous $g_{\mathrm{Ca}} = 0.5$ mS/cm^2. Time and rate parameters are relative to a time constant $\tau = C_m/g_{\mathrm{Ca}} = 2$ ms (since $C_m = 1$ μF/cm^2). The parameter values used here are $g_L = 0.1$, $g_{\mathrm{syn}} = 0.76$, $V_{\mathrm{Ca}} = 1$, $V_L = -0.5$, $V_{\mathrm{syn}} = -0.667$, $k_r = 0.02$, $k_f = 2$, $\phi = 4$, $\theta_m = -0.54$, $\sigma_m = 0.065$, $\theta_h = -0.675$, $\sigma_h = -0.092$, $\theta_s = -0.375$, $\sigma_s = 0.0167$, $\theta_{hk} = -1.35$, $\sigma_{hk} = 0.148$.
[12] M.Tsodyks, I. Mitkov, and H. Sompolinsky, Phys. Rev. Lett. **71**, 1280 (1993).
[13] D. Hansel and H. Sompolinsky, Phys. Rev. Lett. **68**, 718 (1992).
[14] L.F. Abbott and C. Van Vreeswijk, Phys. Rev. E **48**, 1483 (1993).
[15] M.H. Jensen, P. Bak, and T. Bohr, Phys. Rev. A **30**, 1960 (1984); **30**, 1970 (1984); J.P. Keener, F.C. Hoppensteadt, and J. Rinzel, SIAM J. Appl. Math. **41**, 503 (1981).
[16] G.B. Ermentrout and N. Kopell, SIAM J. Math. Anal. **15**, 215 (1984).
[17] T.M. Fisher, M.A.L. Nicolellis, and J.K. Chapin, Neuroscience Abstr. **18**, 1392 (1992).